Journal of Innovative Optical Health Sciences
Vol. 3, No. 4 (2010) 285–292

DOI: 10.1142/S179354581000109X

LESS-INVASIVE LASER THERAPY AND DIAGNOSIS USING A TABLETOP MID-INFRARED TUNABLE LASER

HISANAO HAZAMA*,§, KATSUNORI ISHII* and KUNIO AWAZU*,†,‡
*Graduate School of Engineering, Osaka University
2-1 Yamadaoka, Suita, Osaka 565-0871, Japan
†Research Institute of Nuclear Engineering, University of Fukui
3-9-1 Bunkyo, Fukui, Fukui 910-8507, Japan
‡Institute for Chemical Research, Kyoto University
Gokasho, Uji, Kyoto 611-0011, Japan
§hazama@wakate.frc.eng.osaka-u.ac.jp

Since numerous characteristic absorption lines caused by molecular vibration exist in the mid-infrared (MIR) wavelength region, selective excitation or selective dissociation of molecules is possible by tuning the laser wavelength to the characteristic absorption lines of target molecules. By applying this feature to the medical fields, less-invasive treatment and non-destructive diagnosis with absorption spectroscopy are possible using tunable MIR lasers. A high-energy nanosecond pulsed MIR tunable laser was obtained with difference-frequency generation (DFG) between a Nd:YAG and a tunable Cr:forsterite lasers. The MIR-DFG laser was tunable in a wavelength range of 5.5–10 μm and generated laser pulses with energy of up to 1.4 mJ, a pulse width of 5 ns, and a pulse repetition rate of 10 Hz. Selective removal of atherosclerotic lesion was successfully demonstrated with the MIR-DFG laser tuned at a wavelength of 5.75 μm, which corresponds to the characteristic absorption of the ester bond in cholesterol esters in the atherosclerotic lesions. We have developed a non-destructive diagnostic probe with an attenuated total reflection (ATR) prism and two hollow optical fibers. An absorption spectrum of cholesterol was measured with the ATR probe by scanning the wavelength of the MIR-DFG laser, and the spectrum was in good agreement with that measured with a commercial Fourier transform infrared spectrometer.

Keywords: Mid-infrared tunable laser; difference-frequency generation; selective treatment; attenuated total reflection spectroscopy; hollow optical fiber.

1. Introduction

Since numerous characteristic absorption lines due to the molecular vibration exist in the mid-infrared (MIR) wavelength range, this wavelength range is often termed the molecular fingerprint region. Selective excitation of a molecule is possible by tuning the laser wavelength to the characteristic absorption line of the target molecule. MIR absorption spectroscopy is frequently used for component analysis and structural analysis. By applying these characteristic absorption lines in the MIR wavelength range for the medical field, selective and less-invasive treatments and non-destructive diagnosis are expected to be possible using tunable MIR lasers.

For example, cholesteryl esters, cholesterol bound to fatty acid such as oleic acid via an ester bond, are a principal component of atherosclerotic lesions. Cholesteryl esters have a characteristic absorption line at a wavelength of 5.75 μm, which

originated from the C=O stretching vibration of the ester bond. It has been reported that cholesteryl esters were selectively removed from atherosclerotic lesions by using a free-electron laser (FEL) tuned to a wavelength of 5.75 μm with a pulse width of microseconds.[1–3] Since FEL can generate high-power laser in the MIR wavelength range and is widely tunable, it has been used in various medical applications[4] such as soft tissue ablation,[5] cardiovascular surgery,[1–3] neurosurgery, preventive dentistry,[6] lithotripsy,[7] ophthalmology, and orthopedic surgery. However, extremely large-size and expensive equipments have prevented FEL from the practical applications.

Recently, a tabletop MIR tunable laser using difference-frequency generation (MIR-DFG laser) has been developed.[8,9] The MIR-DFG laser is tunable within a MIR wavelength range of 5.5–10 μm and generates laser pulses with a pulse energy of up to 1.4 mJ, pulse width of 5 ns, and repetition rate of 10 Hz. In general, short pulse lasers in the nanosecond range are more suitable to induce mechanical ablation with suppressing thermal effects compared with pulsed lasers in the microsecond or longer range.[10] In this research, we have evaluated the effectiveness of irradiating the MIR-DFG laser with a wavelength of 5.75 μm for selective and less-invasive treatment of atherosclerotic lesions.

On the other hand, the Fourier transform infrared spectrometer (FT-IR) is one of the most popular spectrometers in the MIR wavelength range. In recent years, it is also applied to the analysis of remote samples by combining attenuated total reflection (ATR) method with optical fibers. This technique can be applied to diagnose a human body and to determine the optimum wavelength for the less-invasive treatment using MIR tunable lasers before the treatment. However, the types of the optical fiber are limited in the MIR wavelength range and the transmittance of the optical fibers for the MIR rays is low compared with that for the visible and near-infrared rays.[11] Since the brightness of the light source used in FT-IR is low, the signal intensity becomes weak by using long optical fibers. In addition, the size of commercial ATR probe is too large to introduce into a human body. In recent years, hollow optical fibers which can transmit MIR rays have been developed.[12–14] By using the hollow optical fibers and the MIR-DFG laser, higher signal intensity is expected compared with FT-IR, and the single laser source can be used for both treatment and diagnosis.

In this paper, our preliminary results of novel therapeutic and diagnostic applications using a tabletop MIR tunable laser are reported. That is, results of *in vitro* experiments for less-invasive laser angioplasty with the MIR-DFG laser at a wavelength of 5.75 μm and ATR spectroscopy of biomolecules performed by scanning the wavelength of the MIR-DFG laser are shown.

2. Experimental Apparatus

2.1. *Mid-infrared tunable laser*

Figure 1(a) schematically depicts the tabletop mid-infrared tunable laser used in this research. The tunable MIR laser in a wavelength range of 5.5–10 μm was obtained by DFG between a Q-switched Nd:YAG laser with a wavelength of 1,064 nm (Tempest 10, New Wave Research, Inc., USA) and

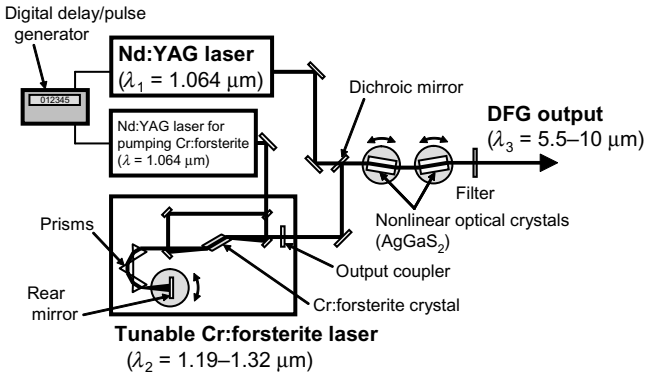

(a)

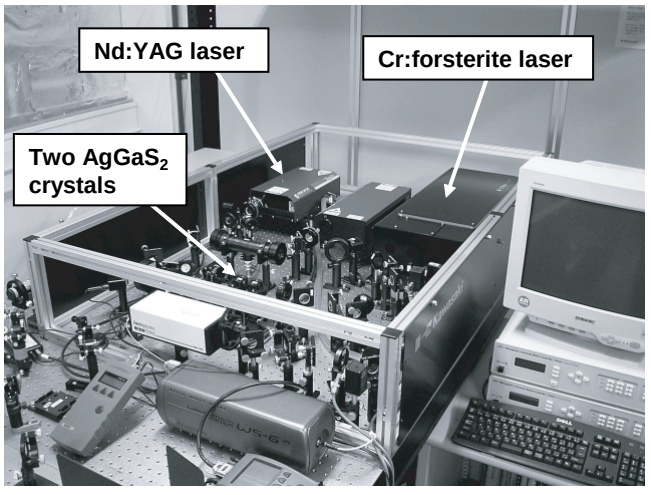

(b)

Fig. 1. Schematic drawing (a) and photograph (b) of the MIR tunable laser. Pulses from two near infrared lasers are combined in two $AgGaS_2$ crystals to produce MIR tunable pulses.

the Cr:forsterite laser tunable within a wavelength range of 1,190–1,320 nm. The wavelength of the Cr:forsterite laser was varied by rotating the rear mirror of the optical resonator and was measured with a wavelength meter (WS6-IR, HighFinesse GmbH, Germany). The wavelength of the MIR output λ_3 was calculated from the wavelengths of the Nd:YAG laser λ_1 and the Cr:forsterite laser λ_2 using the following relationship:

$$\lambda_3^{-1} = \lambda_1^{-1} - \lambda_2^{-1}.$$

The Cr:forsterite laser can be pumped by the fundamental wavelength of the Nd:YAG laser. However, since the buildup time of the Cr:forsterite laser varies from 70 to 200 ns depending on its oscillating wavelength, it is difficult to synchronize the Nd:YAG and the Cr:forsterite laser pulses at the $AgGaS_2$ crystals by using an optical delay. Therefore, a *Q*-switched Nd:YAG laser different from that used for DFG (INDI-40-10, Spectra-Physics, Inc., USA or Tempest 300, New Wave Research, Inc., USA) was used for pumping the Cr:forsterite laser. A digital delay/pulse generator (DG535, Stanford Research Systems, Inc., USA) was used to synchronize the Nd:YAG and the Cr:forsterite laser pulses.

Two $AgGaS_2$ crystals with the same dimensions and the same cutting angles were used to obtain high output energy and to compensate a displacement of the optical axis. The height, width, and length of the $AgGaS_2$ crystals were 9, 12, and 24 mm, respectively. The type II phase-matching condition was used to obtain a higher effective nonlinearity compared with the type I phase-matching.[15]

The prototypes of the tunable MIR laser and the tunable Cr:forsterite laser as a part of the MIR laser were developed by RIKEN and Kawasaki Heavy Industries, Ltd. (KHI). Then, full automation of the wavelength tuning and stabilization of the output energy have been carried out by KHI.

2.2. *ATR probe*

As the diameter of commercial ATR probes is large (>10 mm), we have designed and manufactured an ATR probe. Figure 2 shows a schematic drawing and photograph of the ATR probe. A prism was made of diamond which is chemically stable and not harmful in a human body. Type I b diamond which has weak internal absorption within the wavelength ranges of about 4–6 μm and 7–15 μm was used.[16] Two slanted surfaces of the prism did not satisfy the condition for the total internal reflection, so that the surfaces were coated by nickel to enhance the reflectance. The hollow optical fibers were supplied from J. MORITA MFG Corp. (Kyoto, Japan) or Doko Engineering LLC (Miyagi, Japan). The inner and outer diameters of all the fibers were 700 μm and 850 μm, respectively, and the length of each fiber was up to 2 m. The fibers were made with glass capillaries whose inner surface was coated with silver and cyclic olefin polymer. The fibers can also transmit a visible laser as a guide laser.[12–14] The housing at the tip of the ATR probe holding the diamond ATR prism and two hollow optical fibers was made with polyether ether ketone (PEEK) and the cross-sectional area of the housing was 3.55 mm × 1.05 mm.

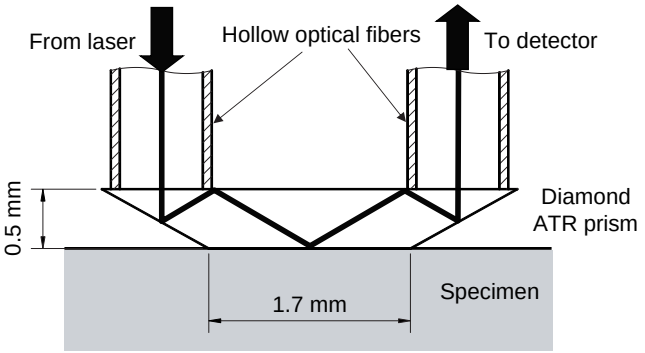

(a)

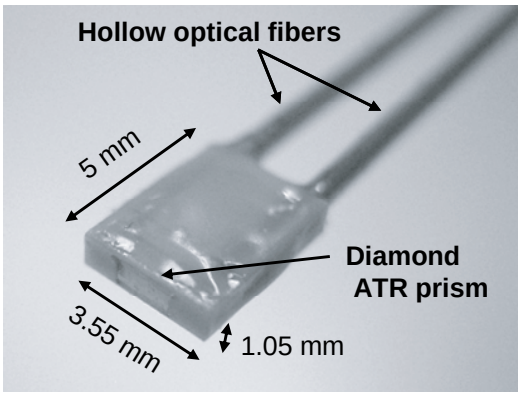

(b)

Fig. 2. Schematic drawing (a) and photograph (b) of the ATR probe comprised of a diamond prism and two hollow optical fibers.

The MIR-DFG laser was focused by an off-axis parabolic mirror with an effective focal length of 150 mm and introduced into one of the two hollow optical fibers attached to the diamond ATR prism. Laser energy came back from the diamond ATR prism via another hollow optical fiber was measured

with a laser energy meter with a detection limit of 0.2 μJ (PE9, Ophir Optronics, Israel).

3. Materials and Methods

3.1. *Animals and sample preparations*

An animal model for spontaneous hypercholesterolemia, coronary atherosclerosis, and myocardial infarction — myocardial infarction-prone Watanabe heritable hyperlipidemic (WHHLMI) rabbits[17,18] — was used as an atherosclerotic model, and Japanese white rabbits were used as a normal model. WHHLMI rabbits (female, 24 months old) were provided by the Institute for Experimental Animals, Kobe University Graduates School of Medicine. Atherosclerotic and normal rabbits were sacrificed by intravenous injection of pentobarbital sodium (50 mg/kg) (Nembutal, Dainippon Sumitomo Pharma Co., Ltd., Japan). Thoracic aortas were excised from the rabbits, rinsed with saline, and stored in saline at 4°C. In order to evaluate the effect of water which has strong absorption in the MIR wavelength range, two kinds of samples, i.e., dry and wet samples were prepared. To prepare the dry samples, the stored aortas were cut into square pieces of 5 mm × 5 mm and dried in air for a day. On the other hand, to prepare the wet samples, the stored aortas were cut into square pieces of 5 mm × 5 mm and immersed in saline, and a BaF_2 window with a diameter of 13 mm and thickness of 1 mm was attached onto the intima. This study was approved by the Institutional Animal Experiments Committee and conducted in accordance with the guidelines of animal experimentation at Osaka University.

3.2. *Laser irradiation and histological analysis*

The MIR-DFG laser was focused using a ZnSe lens with a focal length of 100 mm to a diameter of about 140 μm. Then the laser was irradiated normal to the surface of the thoracic aorta samples from the intimal side. For the wet samples, laser was irradiated through the BaF_2 window attached onto the intima. After laser irradiation, the samples were embedded by Tissue-Tek O.C.T. Compound (Sakura Finetechnical Co., Ltd., Japan). The embedded samples were frozen and sliced by using a cryostat microtome (Leica CM-1850, Leica Microsystems GmbH, Germany) for histological evaluation. Sections were cut vertically to the tissue surface at 10 μm intervals and placed onto glass slides. The sections with a crater produced by laser irradiation were photographed using an optical microscope (DM IRBE, Leica Microsystems) with a cooled color CCD camera (Nebula QICAM, Q Image).

3.3. *Sample preparation for ATR spectroscopy*

Cholesterol (C8667, Sigma-Aldrich, USA) was dissolved in carbon tetrachloride at a concentration of 6×10^{-2} mol/L and the solution with a volume of 5 μL was dropped onto a BaF_2 window with a thickness of 1 mm and diameter of 13 mm. After drying the droplet, an absorption spectrum was measured with ATR spectroscopy and was compared with that measured with a microscopic Fourier transform infrared spectrometer (FT-IR) (FT-520, HORIBA, Japan).

4. Results and Discussion

4.1. *Irradiation effects of the MIR-DFG laser for aorta samples*

Figure 3 shows typical absorption spectra of the atherosclerotic and normal aortas measured using the FT-IR. The absorption peak originated from the C=O stretching vibration of the ester bond in cholesterol esters was observed at the wavelength of 5.75 μm only from atherosclerotic lesions.

Figure 4 shows photomicrographs of the sections of the atherosclerotic and normal aortas after laser irradiation in the dry condition. Tuning the

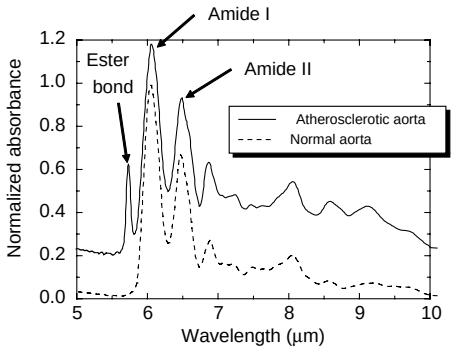

Fig. 3. Typical infrared absorption spectra for the intimal layers of atherosclerotic and normal aortas. The absorption peak originated from C=O stretching vibration of the ester bond in cholesteryl esters was observed at 5.75 μm only from atherosclerotic lesions. (The spectrum for the atherosclerotic aorta is shifted for easier viewing.)

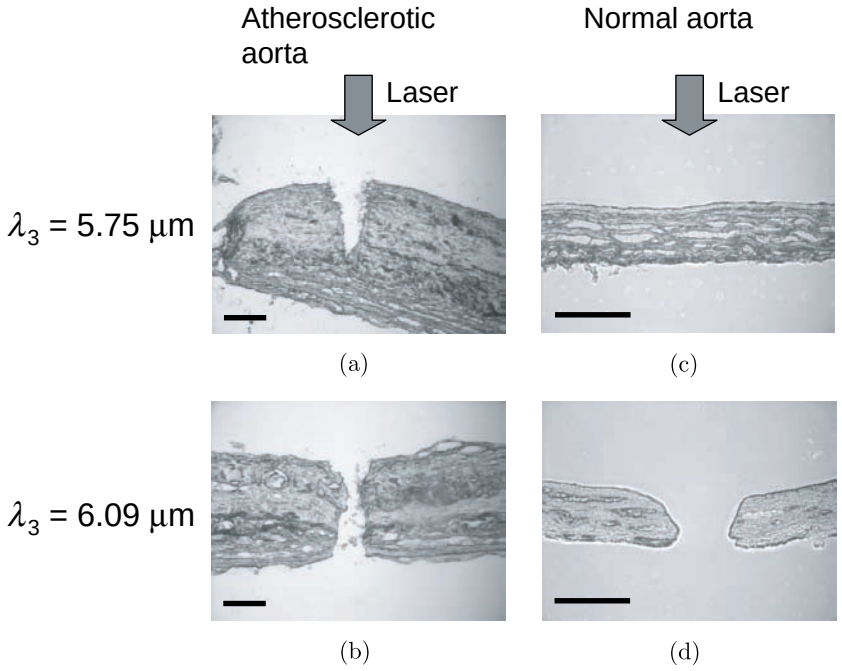

Fig. 4. Photomicrographs of aorta cross-sections after laser irradiation in the dry condition. The top of each image is the intimal layer. When the MIR-DFG laser was tuned to 5.75 μm, the atherosclerotic lesion was removed without damaging normal tissue. Laser exposure time was 3 s (30 pulses) and average power densities were 50 and 40 W/cm^2 for atherosclerotic and normal aortas, respectively. Scale bars at the bottom of each image are 200 μm long.

laser to 5.75 μm allowed selective removal of an atherosclerotic lesion without damaging normal tissue [Figs. 4(a) and 4(c)]. On the other hand, tuning the laser to 6.09 μm, which corresponds to the absorption peak of the amide I band, resulted in perforation of both aortas [Figs. 4(b) and 4(d)]. Therefore, it is suggested that the selective and less-invasive removal of atherosclerotic lesion is possible using the MIR-DFG laser tuned at the wavelength of 5.75 μm.

To evaluate the effectiveness of the irradiation of the MIR-DFG laser with a wavelength of 5.75 μm in more practical cases, aorta samples were irradiated in the wet condition. Figures 5(a)–5(d) and 5(e)–5(h) show photomicrographs of the atherosclerotic and normal thoracic aortas, respectively, where laser was irradiated in the wet condition at the average power density of 80 W/cm^2. Figure 6 shows the ablation depth in Fig. 5 as a function of the laser irradiation time. For both atherosclerotic and normal thoracic aortas, ablation was observed at 1 s and longer irradiation times. However, for all irradiation times, the ablation depth of the atherosclerotic aortas was much larger than that of the normal aortas. Although the normal aortas were damaged by laser irradiation, the ablation depth for the normal aortas remained less than 100 μm, and the rate of increase in the ablation depth became small for irradiation time longer than 10 s. Therefore, severe damage such as perforation will not occur. On the other hand, ultraviolet excimer laser coronary angioplasty (ELCA) is already used in clinical treatment.[19] With ELCA, both atherosclerotic and normal aortas would be ablated at the same rate because the high-energy photons of the XeCl excimer laser at a wavelength of 308 nm ablate tissues by non-selective dissociation of chemical bonds. In the wet condition, laser power density is attenuated due to the absorption by water on the sample surface. For example, water with a thickness of 10 μm absorbs 50% of the laser energy because the absorption coefficient of water at the wavelength of 5.8 μm is 715 cm^{-1}.[20] Although the power densities required to ablate the aortas were higher compared to those required to ablate dry aortas, selective and less-invasive ablation using the MIR laser with a wavelength of 5.75 μm was also successfully demonstrated for wet aortas. The photomicrographs shown in Fig. 5 suggest that the short pulse laser with a pulse width of 5 ns is able to induce mechanical ablation with less-thermal damage.

To perform *in vivo* treatments using MIR lasers, an irradiation fiber was designed and manufactured as shown in Fig. 7. A hollow optical

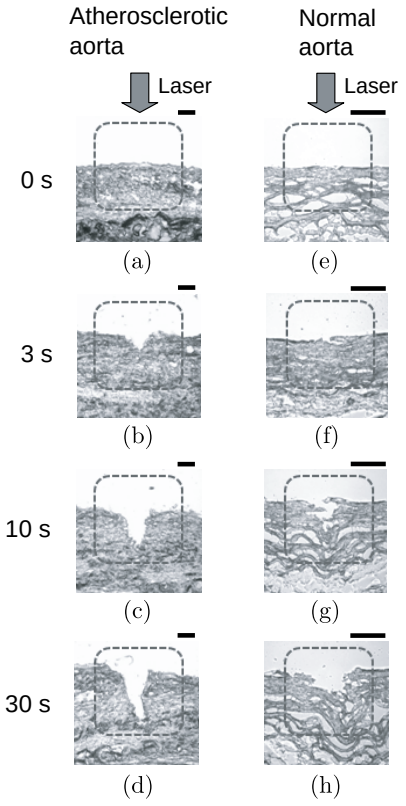

Fig. 5. Photomicrographs of the sections of atherosclerotic and normal thoracic aortas after laser irradiation at a wavelength of 5.75 μm in the wet condition, where the average power density was 80 W/cm^2 and irradiation time was 0–30 s. The top of each image is the intimal layer. Scale bars at the top of each image are 100 μm long.

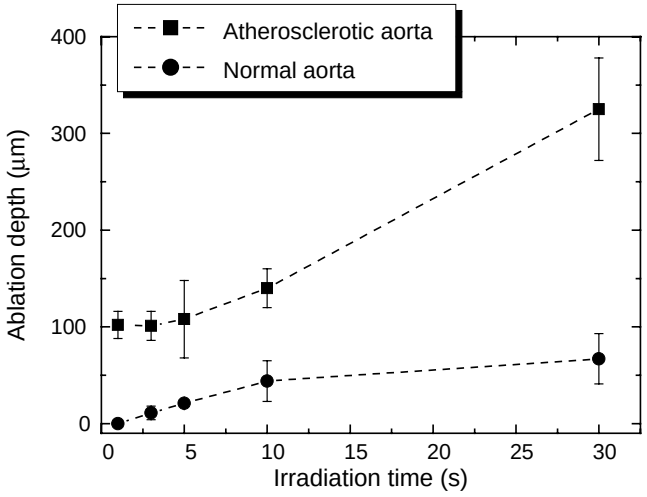

Fig. 6. Ablation depth after laser irradiation with a wavelength of 5.75 μm in the wet condition as a function of the laser irradiation time, where the average power density was 80 W/cm^2. Dots and error bars are the averaged values and the standard deviations from ten samples, respectively.

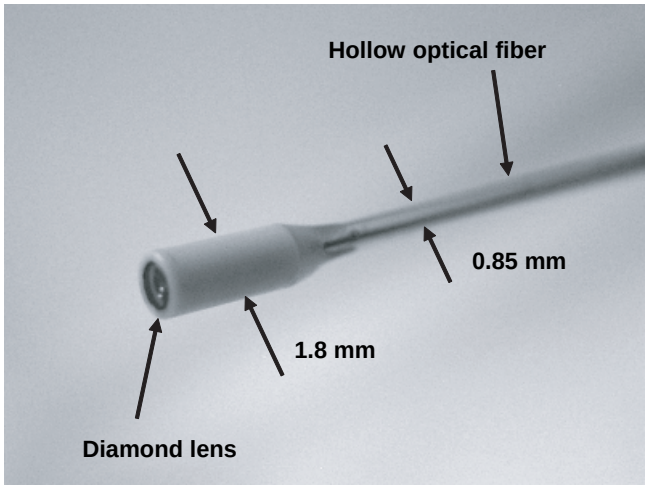

Fig. 7. Photograph of the irradiation fiber developed for less-invasive MIR laser therapy such as angioplasty, lithotripsy, etc. The focal length of the diamond lens was 0.6 mm.

fiber was purchased from Hitachi Cable, Ltd. (Tokyo, Japan), and the specifications of the fiber were the same as those of the fibers used for the ATR probe. Typical transmittance of the hollow optical fiber with a length of 2 m in a straight condition was about 70% at the wavelength of 5.75 μm. A diamond lens with a focal length of 0.6 mm and a diameter of 1.3 mm was attached to the hollow optical fiber using a housing made with PEEK. Since water with a thickness of only 10 μm absorbs 50% of laser energy at the wavelength of 5.75 μm, the exit surface of the diamond lens should tightly be in contact with the surface of lesions. The maximum diameter of the irradiation fiber was 1.8 mm, so that the irradiation fiber can be introduced into blood vessels, digestive organs and so on via a catheter or an endoscope for angioplasty, lithotripsy, etc.

4.2. *ATR spectroscopy*

Figure 5 shows the comparison of absorption spectrum of cholesterol measured with the ATR probe by scanning the wavelength of the MIR-DFG laser and that measured with an FT-IR. In this case, the lengths of the inlet and outlet hollow optical fibers were 85 cm and 35 cm, respectively. Two spectral patterns were in good agreement as shown in Fig. 5. In both spectra, a strong absorption peak caused by the C–H bending vibration was observed at the wavelength of 6.83 μm. Typical transmittance of the ATR probe with a pair of 2 m long hollow optical fibers was about 8% at a wavelength of 6 μm. The

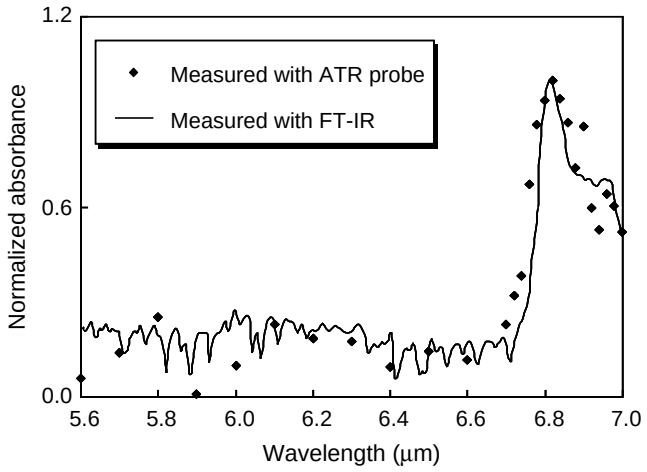

Fig. 8. Infrared absorption spectra of cholesterol measured with the ATR probe and the FT-IR.

tiny ATR probe was made with harmless materials and can be introduced into a human body via a catheter or endoscope. It is supposed that the combination of the ATR probe and the MIR-DFG laser is useful for diagnosis with MIR absorption spectroscopy.

The present control software of the MIR-DFG laser is designed to obtain the best performance for each wavelength by optimizing every parameter, i.e., the angles of the rear mirror of the Cr:forsterite laser and two $AgGaS_2$ crystals and the delay time between the Nd:YAG and Cr:forsterite laser pulses. Under the present circumstances, it takes a few minutes after inputting a wavelength until laser irradiation becomes possible. Therefore, a long time is required to perform the spectroscopic measurement in the wide wavelength range. For example, the measurement of the absorption spectrum in Fig. 8 took about two hours and it was necessary to continuously operate the equipments during the measurement. Thus, we are now developing a new control software to automatically scan the wavelength of the MIR-DFG laser. By using this software, the time required to measure the absorption spectrum in Fig. 8 is estimated to be a few minutes and the whole measurement is performed automatically.

5. Conclusion

The objective of this research was to demonstrate the effectiveness of nanosecond pulsed laser at 5.75-μm irradiation for selective and less-invasive removal of atherosclerotic lesions. *In vitro* experiments using rabbit aortas in both dry and wet conditions showed that the irradiation of nanosecond pulsed laser with the wavelength of 5.75 μm could remove atherosclerotic lesions effectively. In addition, the irradiation effect on normal aortas at the wavelength of 5.75 μm was small. As a result, it was confirmed that less-invasive interaction with normal thoracic aortas could be induced by the wavelength of 5.75 μm, the average power densities of 60–80 W/cm^2 and the irradiation time shorter than 30 s.

We have developed a system for non-destructive and less-invasive diagnosis with the ATR spectroscopy. A tiny ATR probe was developed using a diamond ATR prism and two hollow optical fibers. The absorption spectra of cholesterol were measured with the ATR probe by scanning the wavelength of the tunable MIR laser, and the results were in good agreement with that measured with the FT-IR. The ATR probe can be introduced into a human body via a catheter or endoscope. This fiber-based ATR spectroscopic technique using a high-energy MIR tunable laser realizes the non-labeling chemical diagnosis inside the body, and subsequent selective and less-invasive treatment.

Acknowledgments

This work was supported by Takeda Science Foundation, Japanese Foundation for Research and Promotion of Endoscopy, and Grants-in-Aid for Scientific Research (KAKENHI). The authors thank Dr. Minoru Yokoyama of KHI for his technical cooperation in the experiments using the MIR tunable laser, Prof. Masashi Shiomi of the Institute for Experimental Animals, Kobe University Graduate School of Medicine for providing WHHLMI rabbits, and Mr. Shinya Yamada and Mr. Hideki Tsukimoto for their assistance in the experiments.

References

1. K. Awazu, A. Nagai, K. Aizawa, "Selective removal of cholesterol esters in an arteriosclerotic region of blood vessels with a free-electron laser," *Lasers Surg. Med.* **23**, 233–237 (1998).
2. K. Awazu, Y. Fukami, "Selective removal of cholesteryl oleate through collagen films by MIR FEL," *Nucl. Instrum. Methods Phys. Res. A* **475**, 650–655 (2001).
3. Y. Nakajima, K. Iwatsuki, K. Ishii, S. Suzuki, T. Fujinaka, T. Yoshimine, K. Awazu, "Medical application of an infrared free-electron laser: Selective removal of cholesterol ester in carotid artery

atheromatous plaques," *J. Neurosurg.* **104**, 426–428 (2006).
4. G. S. Edwards, S. J. Allen, R. F. Haglund, R. J. Nemanich, B. Redlich, J. D. Simon, W.-C. Yang, "Applications of free-electron lasers in the biological and material sciences," *Photochem. Photobiol.* **81**, 711–735 (2005).
5. G. Edwards, R. Logan, M. Copeland, L. Reinisch, J. Davidson, B. Johnson, R. Maciunas, M. Mendenhall, R. Ossoff, J. Tribble, J. Werkhaven, D. O'Day, "Tissue ablation by a free-electron laser tuned to the amide II band," *Nature* **371**, 416–419 (1994).
6. M. Heya, S. Sano, N. Takagi, Y. Fukami, K. Awazu, "Wavelength and average power density dependency of the surface modification of root dentin using an MIR-FEL," *Lasers Surg. Med.* **32**, 349–358 (2003).
7. M. Watanabe, H. Kajiwara, K. Awazu, K. Aizawa, "Bilirubin calculi crushing by laser irradiation at a molecular oscillating region wavelength based on infrared absorption spectrum analysis using a free-electron laser: An experimental study," *Surg. Today* **31**, 626–633 (2001).
8. H. Hazama, Y. Takatani, K. Awazu, "Integrated ultraviolet and tunable mid-infrared laser source for analyses of proteins," *Proc. SPIE* **6455**, 645507-1–645507-6 (2007).
9. H. Hazama, K. Ishii, H. Tsukimoto, K. Awazu, "High-energy pulsed tunable mid-infrared laser aids biomedical applications," *SPIE Newsroom*, 10.1117/2.1200801.1000 (2008).
10. M. H. Niemz, *Laser-Tissue Interactions: Fundamentals and Applications 3rd Enlarged Ed.*, Springer, Berlin (2003).
11. J. A. Harrington, *Infrared Fibers and Their Applications*, SPIE Press, Washington (2004).
12. Y. W. Shi, Y. Wang, Y. Abe, Y. Matsuura, M. Miyagi, S. Sato, M. Taniwaki, H. Uyama, "Cyclic olefin polymer-coated silver hollow glass waveguides for the infrared," *Appl. Opt.* **37**, 7758–7762 (1998).
13. Y. W. Shi, K. Ito, Y. Matsuura, M. Miyagi, "Multi-wavelength laser light transmission of hollow optical fiber from the visible to the mid-infrared," *Opt. Lett.* **30**, 2867–2869 (2005).
14. Y. W. Shi, X. S. Zhu, K. R. Sui, X. L. Tang, "Design and fabrication of high-performance infrared hollow fiber for medical laser power delivery," *J. Innov. Opt. Health Sci.* **2**, 101–106 (2009).
15. V. G. Dmitriev, G. G. Gurzadyan, D. N. Nikogosyan, *Handbook of Nonlinear Optical Crystals 3rd Revised Ed.*, Springer, Berlin (1999).
16. J. Walker, "Optical absorption and luminescence in diamond," *Reports Progress Phys.* **42**, 1605–1659 (1979).
17. M. Shiomi, T. Ito, S. Yamada, S. Kawashima, J. Fan, "Development of an animal model for spontaneous myocardial infarction (WHHLMI rabbit)," *Arterioscler. Thromb. Vasc. Biol.* **23**, 1239–1244 (2003).
18. T. Ito, S. Yamada, T. Tamura, M. Shiomi, "Discrimination of recent ischemic myocardial changes in WHHLMI rabbits from the findings of postmortem degeneration," *Exp. Anim.* **54**, 413–419 (2005).
19. R. L. H. Sprangers, G. H. M. Gijsbers, G. K. David, M. Keijzer, J. J. Koolen, M. J. C. Van Gemert, "Excimer laser coronary angioplasty: Initial experience in Amsterdam," *Lasers Med. Sci.* **6**, 281–288 (1991).
20. G. M. Hale, M. R. Querry, "Optical constants of water in the 200-nm to 200-μm wavelength region," *Appl. Opt.* **12**, 555–563 (1973).